



**POLITECNICO**  
MILANO 1863

SCUOLA DI INGEGNERIA INDUSTRIALE  
E DELL'INFORMAZIONE

EXECUTIVE SUMMARY OF THE THESIS

# Environmentally robust Graphene-based transparent antenna for Space-based Solar Power (SBSP) applications

LAUREA MAGISTRALE IN ENGINEERING PHYSICS - INGEGNERIA FISICA

Author: YUVAM BHATEJA

Advisor: DR. EDWARD TATE

Co-advisor: MR. JOHN BUCKNELL, PROF. GUGLIELMO LANZANI

Academic year: 2023-24

## 1. Introduction

The world right now is in a twin problem dilemma. Numerous countries are *Energy Poor*, with millions without electricity or a primary energy fuel. On the other hand, high-GDP nations are over-exploiting global fossil fuel reservoirs. This over-utilization leads to alarming CO<sub>2</sub> emissions. Figure 1 appropriately illustrates the division of the world between energy-hungry and intense CO<sub>2</sub> emitters.

The eminent global warming effect of rising CO<sub>2</sub> in the environment is well known. The world has witnessed a rise in global surface temperature to 1.17° C or 2.11° F as of 2023 compared to the long-term average from 1951 to 1980 [2]. There is an immediate need to pivot the energy dependency over cleaner renewable sources such as Solar, Wind, Hydro, and Nuclear.

According to [3], Hydroelectricity was the primary renewable source with a 44% contribution to the total renewable energy consumption and 14.2% to the global electricity generation in 2023. However, Solar Energy has shown the highest growth rate of 32.2% in 2023, a

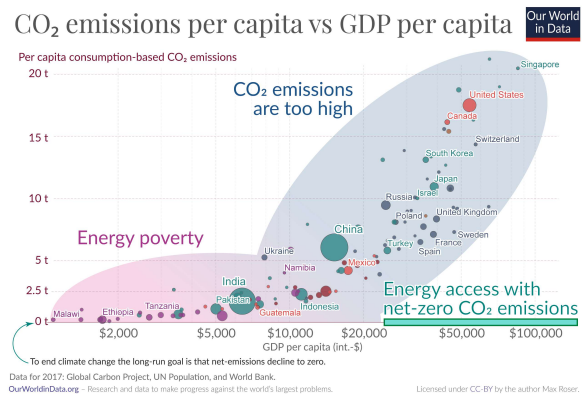


Figure 1: A correlation between per capita CO<sub>2</sub> emissions and GDP per capita for different countries. Based on the World Bank data of 2017. Reproduced with permission from [1].

consistent growth with 24.9% in 2022 and 22.3% in 2021. Several developed nations are targeting the Net-Zero scenario by 2050 with Terrestrial Solar energy as the torch-bearer.

However, harvesting Terrestrial Solar energy poses numerous issues technologically and geographically. A report by [4] discusses a few real-life constraints regarding dependency on Terrestrial Solar energy for the world's energy demand.

It accounts for the constraints to energy extraction, including technological constraints, land use constraints, physical availability constraints, socio-economic scaling constraints, and efficacy of generating systems to deliver energy to society. The reported Energy Return on Investment (EROI) suggests that Terrestrial Solar can yield a maximum of 1099 ExaJoule or 305277.8 TWh per year. This value is 1.77 times the global energy demand as of 2023 [3]. However, with a growing population and technological advancement, the energy demand is increasing at an average rate of 1.4% over the last decade. Considering a 2% annual growth observed in 2023, the world's energy demand tentatively will surpass the Terrestrial Solar energy capacity by 2053. Therefore, it becomes necessary to innovate and integrate new methods of Solar harvesting with the existing ones. Space-based Solar Power is the solution to all these challenges.

## 2. Space-based Solar Power

Space-based Solar Power (SBSP), a concept straight out of fiction, is a method of harvesting Solar energy from space and transmitting it to Earth via a microwave beam. Figure 2 bewitchingly illustrates the complete outline of the SBSP project.

SBSP was first envisioned as a possible energy-harvesting method between the 1970s and 1980s, with NASA conducting several feasibility tests. The concept was technologically viable but deemed costly. High launch costs of that era resulted in an LCOE of \$226.02/MWh after adjusting the current inflation rate for a 2.5GW system. Since then, placing payloads into orbit has gotten cheaper by a factor of at least one hundred. As of 2024, with Virtus Solis SBSP architecture, the LCOE can be less than \$25/MWh, comparable to well-established fossil fuels.

SBSP requires two main components for its realization: a Solar Power Satellite (SPS) to collect Solar power and transmit the transformed microwave power to Earth and a Ground Receiving Station (GRS) to collect and convert the incoming microwave beam into usable electricity. GRS, as shown in point 4 of fig 2, is an assembly of rectenna units spanned over

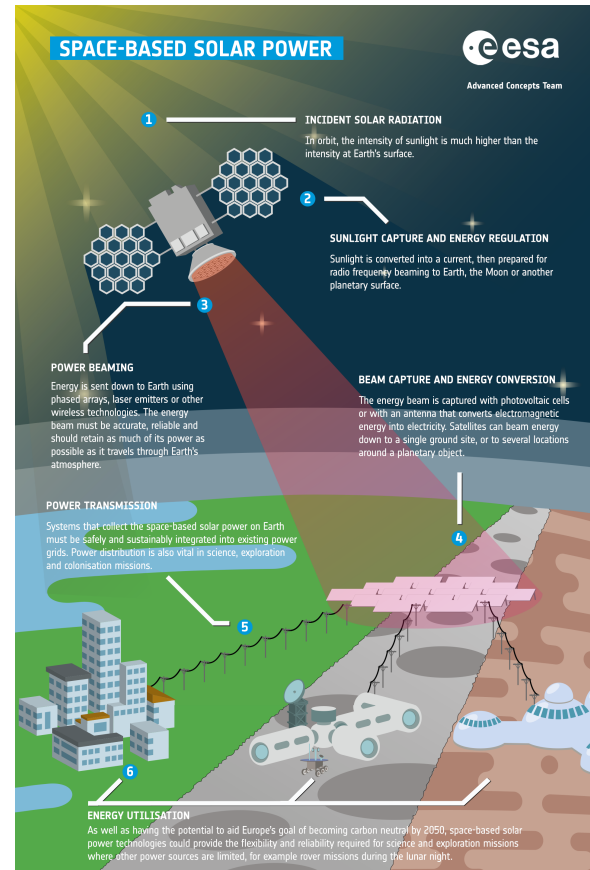


Figure 2: Space-based Solar Power (SBSP). ©ESA.

several km<sup>2</sup> areas. The total area of rectenna arrays will depend on the incoming microwave power density to meet the required capacity. A rectenna is the culmination of an antenna (to convert RF to AC) and a rectifying circuit (to convert AC to DC).

The current work focuses on developing a novel transparent antenna design for the rectenna unit that is both environmentally robust and compatible with photovoltaic (PV) cell integration. The environmental robustness establishes the superiority of rectenna cells over conventional PV cells. Moreover, this integration will tentatively lower the Levelized Cost of Energy (LCOE) of SBSP.

## 3. Transparent Antenna

The net capital and operation costs of large-scale solar farms are heavily driven by their footprints. For example, the largest solar farm in existence - Bhadla Solar Park, located in Rajasthan India, with a capacity of 2.245 GW, spanned over 56 km<sup>2</sup> area. Therefore, it is necessary to optimize

the power per square meter generated to reduce the final Levelized Cost of Energy (LCOE). On a contrary, an advanced Space-based Solar Power (SBSP) architecture (sans integration), can deliver a 8 GW power to the grid with only a requirement of 14.9 km<sup>2</sup> area. Integration between the rectenna farm, constituting one-half of the SBSP project, to the existing solar farms at a much lower cost without expanding the already occupied land will substantially elevate the generated power per square meter. Such integration will undoubtedly reduce the final Levelized Cost of Energy (LCOE). However, successful integration hinges on developing an efficient transparent antenna compatible with the Vitus Solis rectenna circuit units.

### 3.1. Methodology

The current work consists of numerical modelling performed in Ansys HFSS to analyze patch antennae for single-element and large periodic array (infinite array) configurations.

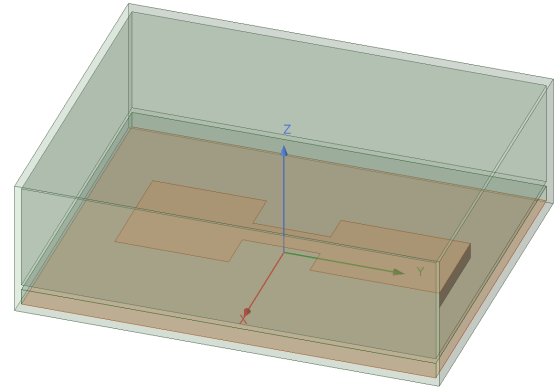
The proposed antenna design features two enclosed hollow glass boxes merged into a single structure with graphene antenna elements (antenna and ground plane) fabricated onto the inner surfaces of the bottom glass box. The bottom glass box has a gap of thickness 0.1575 cm filled with air/vacuum that serves as the antenna substrate. Similarly, the top glass box has an air/vacuum gap of thickness of 1.04 cm. The glass thickness is kept at 0.05 cm to minimize dielectric power losses in the glass material. These thin glasses are commercially available and commonly used in everyday applications such as, but not limited to, tempered glass for smartphones. For the current discussion, a predefined glass material with a relative permittivity of 5.5 is chosen from the HFSS library. The antenna structure is shown in fig 3.

Due to the finite width, a microstrip experiences a fringing effect from its edges. Fringing makes the microstrip line look wider electrically compared to its physical dimensions. Since some of the waves travel in the substrate and some in the air, an effective dielectric constant  $\epsilon_{eff}$  is introduced to account for fringing and wave propagation in the line. This  $\epsilon_{eff}$  for a system

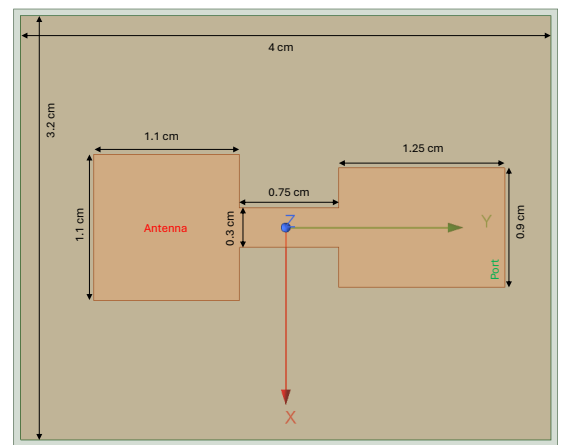
of a dielectric substrate and radiating medium air can be calculated by [5]:

$$\epsilon_{eff} = \frac{\epsilon_r + 1}{2} + \frac{\epsilon_r - 1}{2} \left[ 1 + 12 \frac{h}{W} \right]^{-1/2}, \quad (1)$$

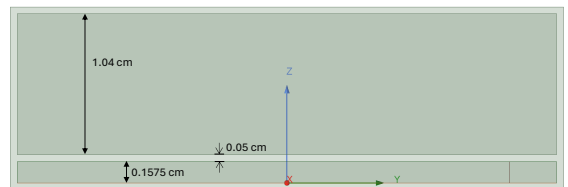
where  $\epsilon_r$  is the relative permittivity of the substrate,  $h$  is the substrate thickness, and  $W$  is the width of the radiating patch.



(a) Dimetric View.



(b) Top View.



(c) Side View (partial).

**Figure 3:** Ansys HFSS model of graphene antenna with air substrate enclosed within glass box.

However, the proposed design involves glass sheets above and below the antenna, creating

a multi-level superstrate structure. This necessitates calculating the effective permittivity differently (referred to [6, 7] for direction) during antenna parameters estimation, later fine-tuned, to achieve optimal performance at 10 GHz, as shown in fig 3b. This concept aligns with the findings in [7] that proposed the enhanced performance by incorporating single and multiple superstrates with high dielectric, which is observed in the currently proposed design and further discussions.

For the infinite array configuration, the system parameters are set in a following way including certain approximation for an optimum trade-off between the performance and computational expense.

- The topmost face of the air box is kept more than 1.5 cm (half a wavelength) away from the radiating patch, and the bottom-most one is 0.75 cm (quarter of a wavelength) away from the ground element. However, there is no gap between the air box surfaces and the antenna laterally to create a periodic lattice structure.
- The periodicity is introduced using Primary-Secondary boundary conditions on the opposite surfaces combined with a Floquet port on the topmost surface of the air box. The airbox takes the dimensions of 3.3 cm  $\times$  4.1 cm  $\times$  2.5075 cm, with radiating boundary conditions applied to the remaining sides.
- A fine mesh with a maximum element size of 0.5 cm is used for accurate results.
- The antenna is subjected to a 50  $\Omega$  port with a model solution type, which is required to utilize the Floquet port.

### 3.2. Environmental Testing

Large solar farms experience power loss of more than 50% within four months of operation (without any rainy days) if kept uncleaned. Therefore, they require a large amount of water for cleaning, around 20 gal/MWh. On the contrary, microwave rectenna poses a significant advantage over photovoltaics (PVs) in terms of environmental robustness since the dust and debris do not strongly interact with the microwave frequencies at which SBSP operates. However, water is one of the greater nemesis of

microwave frequencies. Water behaves aggressively within this frequency range, which is how the microwave oven works. Water has a high dielectric constant, real and imaginary, at 10 GHz, which suggests a significant perturbation in the effective dielectric of the antenna and power losses. Therefore, it is essential to test the antenna performance against these phenomena.

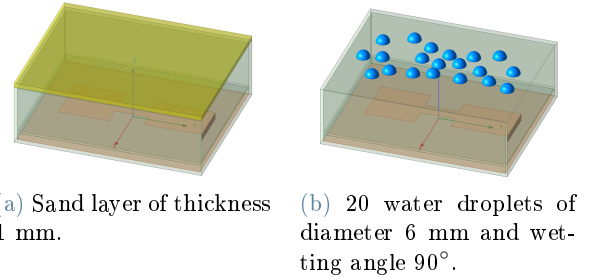


Figure 4: Numerical model of sand layer and water droplets on top of newly proposed Graphene antenna with air gap.

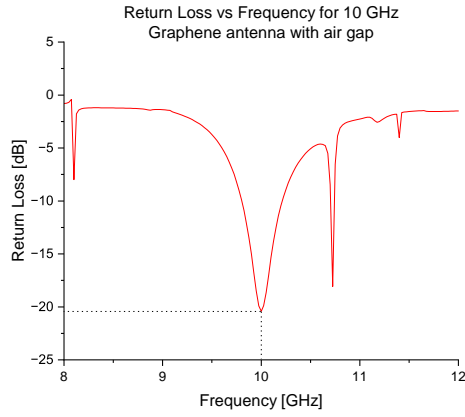
To simulate dust buildup, the sand layer is virtually stacked on the proposed antenna structure with increasing thickness from 0.1 mm to 1 mm. Similarly, for rain, twenty water spheres with different radii and segments are stochastically placed over the top glass surface. This proposed setup will closely mimic different droplet sizes and wetting angles for a thorough analysis. For the current study, the droplet sizes (diameters) are varied from 1 mm to 6 mm, with wetting angles swept from 30 to 120 degrees.

### 3.3. Results

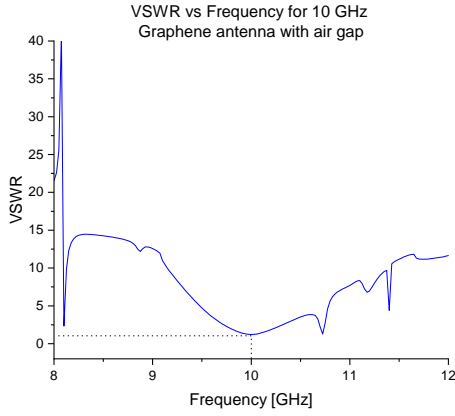
The proposed antenna was simulated for both unit cell and infinite array configuration. However, since the antenna needs to be constructed into large arrays, it is essential to focus more on the results obtained from infinite array configuration.

The proposed antenna works at a 96.457% efficiency with a peak gain of 10.16 dB at 10 GHz in the direction normal to the antenna plane. Referring to the gain pattern as shown in fig 6, it is evident that the occurrence of an additional side lobe is due to a mutual coupling between the elements. The large array configuration also displays an efficient impedance matching of the antenna with the 50  $\Omega$  port. The resultant

return loss and VSWR values at 10 GHz are -20.41 dB and 1.21, respectively (refer to fig 5).



(a) Return Loss.

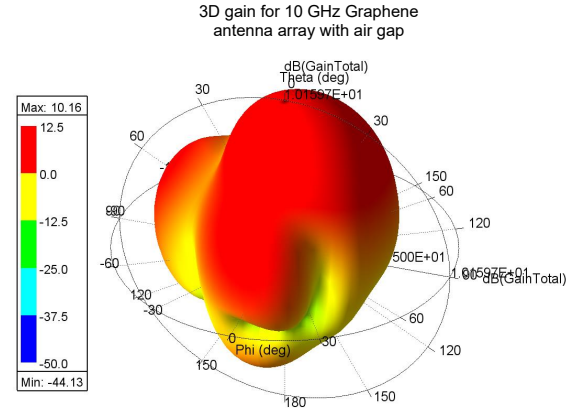


(b) 2D Gain.

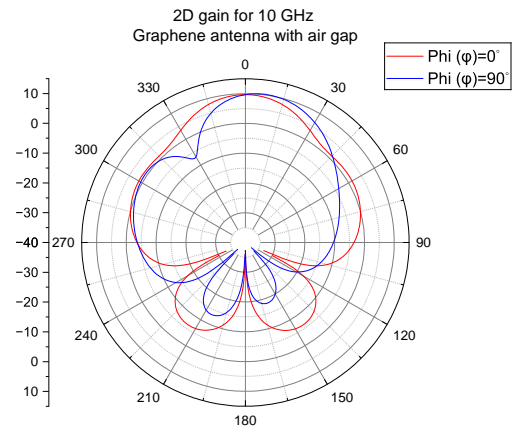
Figure 5: Return loss and VSWR of Graphene-based transparent infinite array with air gap.

After analysing the sand deposition, it was observed that the maximum power loss incurred is 6.23% at 1 mm of thickness, equivalent to over 100 years of uninterrupted sand and debris deposition. This lack of need for cleaning the rectenna farms makes it superior to conventional Solar farms.

Water causes tremendous issues in microwave devices, especially at our current frequency of interest, 10 GHz. However, the new proposed design showcases a maximum power loss of a mere 4.94 % with the 20 droplets of 6 mm and  $90^\circ$  wetting angle. The remarkable robustness (as shown in fig 7) of the antenna performance against the sand and rain is because of the air gap on top of the radiating Graphene patch. The



(a) 3D gain.



(b) 2D Gain.

Figure 6: 3D gain and 2D gain of Graphene-based transparent infinite array with air gap.

gap of 1.04 cm allowed undesired depositions to steer out of the Near-field of the antenna and, therefore, not perturb its performance.

## 4. Conclusions

The current work proposed a transparent Graphene-based antenna compatible with Virtus Solis' proprietary rectifying circuit. The antenna operates at the 10 GHz frequency. The transparency of the antenna unit allows for integration with the PV cell without deteriorating either of the devices' performances. The final design of the proposed antenna includes graphene-based radiating patches enclosed within a glass box. The assembly of 0.5 mm thick glass sheets as a box allows for an air substrate of a height of 0.1575 cm. The design also includes an air gap of 1.04 cm on top of the antenna to prevent contaminations from perturbing the antenna's near-field.

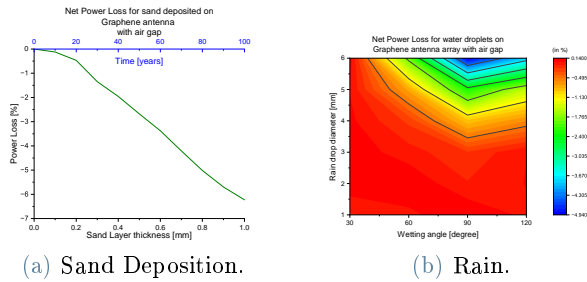


Figure 7: The net power loss incurred in the operation of transparent Graphene antenna due to the sand deposition and water droplets on top of it.

The proposed antenna underwent testing to evaluate its resilience against sand deposition and water droplets of different sizes and wetting angles. Appropriate numerical models were designed within the Ansys HFSS to replicate realistic environmental conditions. The antenna displayed remarkable robustness with just 6% power loss for the sand layer equivalent to a century-long continuous deposition. Similarly, 20 water droplets of different sizes and wetting angles on top of the antenna could only produce a maximum of 4.9% power loss. These results indicate the remarkable robustness of the antenna towards environmental factors and is suitable for GRS.

## 5. Acknowledgements

The author of this report is fortunate to have this opportunity of immense learning and understanding of one of the most revolutionary technologies. The author would like to thank Mr John Bucknell, CEO of Virtus Solis Inc. and Dr Edward Tate, CTO of Virtus Solis Inc., for allowing him to conduct this work and providing the necessary resources and their continuous guidance.

The author is also grateful to Prof Guglielmo Lanzani of the Department of Physics, Politecnico Di Milano, for his continuous support in this work as his academic supervisor and mentor. Prof Lanzani also taught the author the subject ‘Process of Photovoltaics,’ which helped him gain the necessary knowledge and inspired him to undertake this project.

The author also expresses his gratitude to Prof Matteo Oldoni of the Department of Electronics, Information and Bioengineering,

Politecnico Di Milano. Lengthy discussions with Prof Oldoni helped the author understand the theoretical concepts necessary for this work. Those discussions also covered some bottleneck issues with the most industrially accepted software.

In conclusion, the author would like to express his sincere gratitude to his family and friends for their unwavering motivation and support throughout this endeavour.

## References

- [1] Max Roser. The world’s energy problem. *Our World in Data*, 2020. <https://ourworldindata.org/worlds-energy-problem>.
- [2] Global temperature, Feb 2024. URL <https://climate.nasa.gov/vital-signs/global-temperature/?intent=121>.
- [3] Statistical review of world energy. URL [https://www.energyinst.org/\\_data/assets/pdf\\_file/0006/1542714/EI\\_Stats\\_Review\\_2024\\_single\\_pages.pdf](https://www.energyinst.org/_data/assets/pdf_file/0006/1542714/EI_Stats_Review_2024_single_pages.pdf).
- [4] Elise Dupont, Rembrandt Koppelaar, and Hervé Jeanmart. Global available solar energy under physical and energy return on investment constraints, January 2020. URL <http://dx.doi.org/10.1016/j.apenergy.2019.113968>.
- [5] Constantine A. Balanis. *Antenna theory: Analysis and design*. John Wiley & Sons, Incorporated, 2016.
- [6] Dinesh Rano and Mohammad S. Hashmi. Determination of effective dielectric constant and resonant frequency of microstrip patch antenna with multilayered superstrate structures, October 2019. URL <http://dx.doi.org/10.23919/EuMC.2019.8910736>.
- [7] Niamat Hussain, Uktam Azimov, Minjoo Jeong, Seungyeop Rhee, Seung W. Lee, and Nam Kim. A high-gain microstrip patch antenna using multiple dielectric superstrates for wlan applications. *Applied Computational Electromagnetics Society Journal*, 35 (2):187–193, February 2020. ISSN 1054-4887. Publisher Copyright: © ACES.